

RADIO EMISSION FROM THE DOUBLE-PULSAR SYSTEM J0737–3039 REVISITED

S. CHATTERJEE,¹ W. M. GOSS,² AND W. F. BRISKEN²

Received 2005 September 16; accepted 2005 October 13; published 2005 November 4

ABSTRACT

The double pulsar J0737–3039 is the only known system in which the relativistic wind emitted by a radio pulsar demonstrably interacts with the magnetosphere of another one. We report radio interferometric observations of the J0737–3039 system with the VLA at three wavelengths, with each observation spanning a full binary orbit. We detect J0737–3039 at 1.6 and 4.8 GHz, derive a spectral index of -2.3 ± 0.2 , and place an upper limit on its flux density at 8.4 GHz. Orbital modulation is detected in the 1.6 GHz data, with a significance of $\sim 2 \sigma$. Both orbital phase-resolved and phase-averaged measurements at 1.6 GHz are consistent with the entire flux density arising from the pulsed emission of the two pulsars. Contrary to prior results, we find no evidence for unpulsed emission, and limit it to less than 0.5 mJy (5σ).

Subject headings: pulsars: individual (J0737–3039A, J0737–3039B) — stars: neutron

1. INTRODUCTION

The double pulsar J0737–3039 is one of the most extraordinary systems in all of astronomy. It consists of a recycled pulsar (“A”; Burgay et al. 2003) with a period of 22.7 ms in a 2.4 hr eccentric binary orbit ($e = 0.09$), with a young pulsar (“B”; Lyne et al. 2004) that has a 2.8 s period. Since both neutron stars in the highly relativistic binary system are detected as radio pulsars, unprecedented tests of theories of gravitation are possible. In addition, the orbit is tight enough that the relativistic wind from A interacts with the magnetosphere of B, providing a unique laboratory for studying the energy dissipation of neutron stars.

The J0737–3039 system offers an astonishing variety of observational surprises (Lyne et al. 2004). The wind from A apparently regulates the pulsed emission from B, which is bright only at certain parts of its orbit. (In fact, this intermittency was responsible for B not being detected simultaneously with A.) Single pulses from B show features drifting at the beat frequency between the periods of the two pulsars, reflecting the direct impact of electromagnetic radiation from A on B (McLaughlin et al. 2004b). Meanwhile, since the plane of the orbit is almost edge-on to our line of sight, A undergoes a short eclipse (Lyne et al. 2004; Kaspi et al. 2004) when it passes behind B. In a remarkable analysis, McLaughlin et al. (2004c) showed that the eclipse of A is modulated at half the rotational period of B, and ascribed the phase-dependent opacity to synchrotron absorption in a cometary magnetosheath (as suggested by Arons & Spitkovsky 2004) that surrounds and rotates with B. More recently, Lyutikov & Thompson (2005) suggest that relativistically hot dense plasma confined by the magnetic field of pulsar B scatters emission from A at synchrotron resonance, leading to the observed phase-dependent opacity.

Based on an ATCA (Australia Telescope Compact Array) observation, Burgay et al. (2003) reported that the radio flux density from J0737–3039 was 6.9 ± 0.6 mJy at 1.4 GHz. (As is standard practice, all pulsar flux densities discussed here are averaged over pulse phase.) With the discovery of B, Lyne

et al. (2004) measured individual pulsar flux densities of 1.6 ± 0.3 mJy for A and $(0-1.3) \pm 0.3$ mJy for B, for an orbital phase-averaged pulsed flux density of ~ 1.8 mJy at 1.4 GHz. They suggested that the remaining ~ 5 mJy was unpulsed emission that arose from the interaction of the relativistic winds of A and B. Such an interaction also provides a possible explanation for the X-ray emission from the system, as detected by *Chandra* in a brief (10 ks) observation (McLaughlin et al. 2004a). Somewhat deeper *XMM-Newton* observations (Campana et al. 2004; Pellizzoni et al. 2004) show no evidence for any modulation in the X-ray emission, and the existing X-ray data do not necessarily require interaction between the two pulsars, but deeper observations (planned for late 2005) will be required for a definite conclusion.

Much theoretical effort has gone into interpreting the unusual richness of behavior exhibited by J0737–3039 (e.g., Lyutikov 2004; Demorest et al. 2004). Arons & Spitkovsky (2004) suggest that the unpulsed radio emission from J0737–3039 may be synchrotron emission from the magnetosheath of B, enhanced by gyrophase bunching, while Turolla & Treves (2004) propose that it arises either from a shock-heated electron cloud, or from a bow shock surrounding B’s cometary magnetosheath. Either scenario has interesting implications for our understanding of relativistic winds from neutron stars. We note, however, that the existence of unpulsed emission is not required by models (e.g., Lyutikov & Thompson 2005).

In this Letter we report radio interferometric observations of the J0737–3039 system with the NRAO Very Large Array (VLA) at three frequency bands, with each observation spanning a full pulsar orbit. Interferometric observations are sensitive only to the total system flux density, which we determine at 1.6 and 4.8 GHz and limit at 8.4 GHz. We derive a spectral index ($S_\nu \propto \nu^\alpha$, $\alpha = -2.3 \pm 0.2$), which is consistent with radio emission from pulsars, but steeper than that expected for a pulsar wind nebula. There is no evidence for extended structure, as might be expected for a pulsar wind nebula. At 1.6 GHz, we detect modulation due to the orbital phase-dependent emission from B (with a significance of $\sim 2 \sigma$) and find upper limits on the system flux density when A is in eclipse. Crucially, the entire flux density at 1.6 GHz can be accounted for by the sum of pulsed flux densities from A and B, as reported by Lyne et al. (2004). Thus, there is *no evidence for unpulsed radio emission* from the system. Each aspect is discussed in detail below.

¹ Jansky Fellow, National Radio Astronomy Observatory; and Harvard-Smithsonian Center for Astrophysics, 60 Garden Street, Cambridge, MA 02138; schatterjee@cfa.harvard.edu.

² National Radio Astronomy Observatory, P.O. Box O, Socorro, NM 87801; mgoss@aoc.nrao.edu, wbrisken@aoc.nrao.edu.

TABLE 1
SUMMARY OF OBSERVATIONS

Date	Array	ν (MHz)	$\Delta\nu$ (MHz)	T_{int} (hr)	Beam (arcsec)	P.A. (deg)	S_ν (mJy)	σ_ν (mJy)
2003 Jun 28	ATCA	1384	104	4.8	10.6×4.7	-12.2	1.83	0.34
2004 Aug 01	VLA B	1465	20	0.7	12.0×3.5	-0.7	2.28	0.18
2005 Nov 28	VLA A	1666	20	2.2	2.25×0.82	4.0	1.88	0.10
2005 Nov 29	VLA A	4885	44	2.2	1.33×0.37	-10.4	0.17	0.03
2005 Nov 30	VLA A	8435	44	2.0	0.33×0.26	0.2	...	0.02

NOTE.— T_{int} is the total on-source integration time, while the span of the data is longer. P.A. is the beam position angle, measured east of north.

2. FLUX DENSITY AND SPECTRAL INDEX

J0737–3039 was observed with the VLA in its widest configuration (A array) on 2004 November 28, 29, and 30 at 1.6, 4.8, and 8.4 GHz, respectively, with observations spanning a full binary orbit on each day. The observational parameters are summarized in Table 1. In each case, 3C147 was observed as the primary flux density calibrator, and a nearby compact extragalactic source was employed as a phase calibrator and secondary amplitude calibrator. At 1.6 GHz, we employed J0738–3322 (2°7 away), while J0747–3310 (3°2 away) was used at 4.8 and 8.4 GHz.

The data were processed within AIPS, the Astronomical Image Processing System. The steps included data flagging to excise radio-frequency interference, setting the flux density scale based on observations of 3C147, and determining antenna gains and phases from scans on the secondary calibrator. At 1.6 GHz, two passes of self-calibration were employed, with all detected sources within the primary beam included in the model. The positions and flux densities of all strong sources in the field are listed in Table 2.

J0737–3039 was detected at 1.6 and 4.8 GHz, and we fit elliptical Gaussians to the images (task JMFIT in AIPS) to determine the source position and flux density. The source flux density is 1.88 ± 0.10 mJy at 1.6 GHz and 0.17 ± 0.03 mJy at 4.8 GHz, which leads to a spectrum $S_\nu \propto \nu^\alpha$, $\alpha = -2.3 \pm 0.2$, as plotted in Figure 1. At 8.4 GHz, we do not detect the pulsar, but place an upper limit of 0.06 mJy

(3 σ) on its flux density. As shown in Figure 1, such an upper limit is consistent with the measured spectral index.

3. ORBITAL MODULATION OF THE RADIO EMISSION

The shortest integration time possible at the VLA is 1.66 s, so that the rotational phase of either pulsar A or B is impossible to resolve. However, the 1.6 GHz VLA observations have sufficient signal-to-noise ratio (S/N) to permit estimates of the system flux density over several bins in binary orbital phase. Based on the observations presented by Burgay et al. (2005), B is expected to be detectably brighter (i.e., to cause the J0737–3039 system to have a detectably higher flux density) between orbital phases of $\sim 274^\circ$ and 297° , and brightest between $\sim 196^\circ$ and 224° , at the time of our VLA observations (2004 November). Meanwhile, A undergoes its brief eclipse at an orbital phase of 90° . (In each case, orbital phase is measured as the sum of the longitude of periastron and the true anomaly of the respective pulsars, so that A and B are always 180° apart in their orbital phase.)

In order to estimate the flux density of J0737–3039 over bins in orbital phase, all the field sources first have to be accounted for. An interferometer samples different points in the visibility (spatial frequency) plane as the Earth rotates over the course of an observation, leading to a time-varying beam pattern. We account for this effect by first imaging the entire data span (as described above) and then subtracting the modeled contributions of each background source from the interfero-

TABLE 2
SOURCES IN THE FIELD OF J0737–3039 AT 1.6 GHz

R.A. (J2000.0)	Decl. (J2000.0)	Flux Density (mJy beam $^{-1}$)	$\Delta\theta$ (arcmin)	Comment
07 37 51.248	-30 39 40.83	1.9	0.00	Pulsar
07 37 51.075	-30 44 03.55	2.0	4.38	Compact double
07 37 48.034	-30 33 33.90	0.8	6.15	
07 37 52.411	-30 47 11.04	1.2	7.51	
07 37 44.819	-30 48 55.55	0.5	9.35	
07 38 30.425	-30 46 49.25	2.2	11.04	
07 38 43.344	-30 40 40.16	1.4	11.25	
07 38 40.997	-30 44 45.52	5.6	11.84	
07 38 46.237	-30 36 50.10	2.3	12.17	Extended double
07 37 42.214	-30 27 19.34	3.3	12.51	
07 36 51.230	-30 37 46.16	3.3	13.05	
07 37 44.153	-30 54 36.49	1.3	15.00	
07 37 09.591	-30 27 10.19	146	15.39	Partly resolved
07 38 19.790	-30 25 05.23	1226	15.83	Partly resolved
07 36 45.369	-30 27 18.78	18	18.82	

NOTE.—Units of right ascension are hours, minutes, and seconds, and units of declination are degrees, arcminutes, and arcseconds. Flux densities are from VLA A-array observations at 1.6 GHz, and an epoch of MJD 53,337, corrected for the effects of the primary beam. $\Delta\theta$ is the angular offset in arcminutes from the pulsar position. Absolute positions are accurate to $\sim 0''.05$.

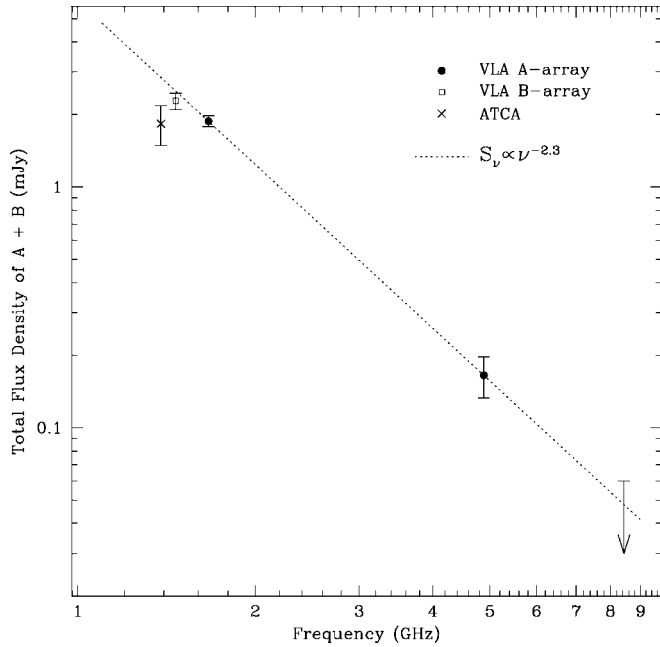
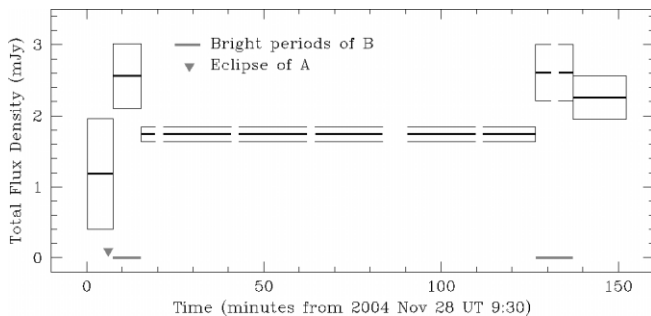


FIG. 1.—Spectrum of J0737–3039. With VLA A-array observations spanning a full binary orbit at each frequency, we determine source flux densities of 1.88 ± 0.10 mJy at 1.6 GHz and 0.17 ± 0.03 mJy at 4.8 GHz, and place a 3σ upper limit of 0.06 mJy at 8.4 GHz. A spectral fit is shown based on the two detections. In addition, detections of J0737–3039 in archival data from VLA B-array and ATCA observations at 1.4 GHz are also plotted. The flux density determinations from archival data are consistent with the derived spectrum (see discussion in § 4).

metric visibilities. The remainder consists of the contributions of the two pulsars, A and B, along with the thermal noise and any systematic errors due to unmodeled source contributions.³ These residuals were binned in time, using published pulse timing solutions (Lyne et al. 2004) to predict the orbital phase as observed from the VLA. Finally, images were created from the data in each time bin, and an elliptical Gaussian at a known (fixed) position was fit to the image to determine the flux density of J0737–3039.

Orbital phase-resolved flux densities at 1.6 GHz are plotted in Figure 2. We find that the flux density of the J0737–3039 system (A+B) is 2.6 ± 0.4 mJy when B is brightest (orbital

³ Such errors may arise, for example, due to modulation of strong sources near the edge of the primary beam, because of pointing errors.



phase $\sim 196^\circ$ – 224°), 2.6 ± 0.5 mJy when it is weakly detectable, and 1.7 ± 0.1 mJy when it is faint and only A is expected to be visible. These estimates are completely consistent with the measurements of Lyne et al. (2004), as listed in § 1. We also created short time bins at and around the eclipse of A. While J0737–3039 was not detected in the bin corresponding to the eclipse of A, we lack the S/N to place a significant upper limit on the total flux density in that short (~ 1 minute) time interval.

4. DISCUSSION: IS THERE UNPULSED RADIO EMISSION?

At 1.6 GHz, we find an orbital phase-averaged flux density of 1.88 ± 0.10 mJy for J0737–3039, consistent with the sum of the pulsed emission from A and (intermittently) B. Our phase-resolved measurements are also consistent with this picture. After subtracting the pulsed flux density (~ 1.8 mJy; Lyne et al. 2004), there is no evidence for any unpulsed flux, and we can rule out the existence of unpulsed emission at the 0.5 mJy level (5σ).

Given the discrepancy with previous work, we have examined the archival ATCA data that form the basis for the claimed unpulsed emission, as well as archival VLA B-array data at 1.4 GHz (see Table 1). The VLA B-array data span only 40 minutes (when B spans an orbital phase range of 96° to 197°), and after standard calibration, we find a flux density of 2.3 ± 0.2 mJy for J0737–3039. As shown in Figure 1, this is consistent with the spectrum derived from 1.6 and 4.8 GHz VLA A-array observations. There is also no evidence for any extended structure, and the mean flux density is $<30 \mu\text{Jy beam}^{-1}$ in an annulus between $10''$ and $100''$ from the pulsar.

The ATCA data were calibrated within MIRIAD and then imaged in AIPS. Due to limited coverage of the visibility plane, the data are comparatively more difficult to self-calibrate and image. After discarding data in the inner visibility plane and only retaining data between 5 and 20 kλ, we find a flux density of 1.8 ± 0.3 mJy for J0737–3039, inconsistent with the value of 6.9 ± 0.6 mJy reported by Burgay et al. (2003). We suggest three possible causes for the discrepancy: (1) there are many sources in the field (Table 2), and it is possible, though unlikely, that the flux density may have been transcribed for an incorrect one; (2) the ATCA data on J0737–3039 were acquired in pulsar-binning mode, while data on the calibrators (B1934–638 and B0727–365) were acquired in the standard mode, necessitating the scaling of amplitudes to obtain correct flux densities. We have averaged all the pulsar bins in our

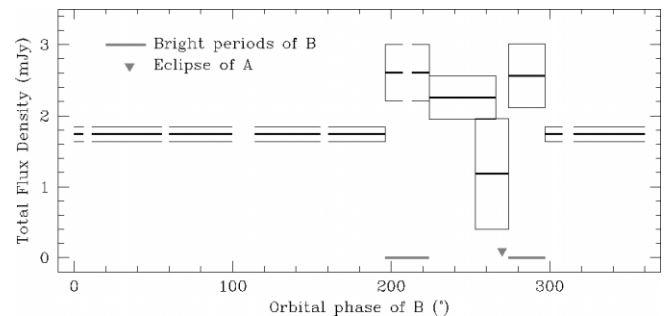


FIG. 2.—Light curve of J0737–3039 at 1.6 GHz, as a function of time (left) and orbital phase of B (right). The flux density is indicated (thick line) along with $\pm 1\sigma$ errors on the measurement (thin lines). The observations span slightly more than a full orbit, with gaps corresponding to interleaved calibration scans. The times and phases when B is expected to be brighter are identified. The flux density varies from 2.6 ± 0.4 to 1.7 ± 0.1 mJy, due to the expected variability of pulsar B, which we thus detect at the $\sim 2\sigma$ level. J0737–3039 is not detected during the ~ 1 minute eclipse of A (when A is at an orbital phase of 90° , and B is at a phase of 270° , as marked), but we lack the S/N to derive significant upper limits on the flux density in that interval.

analysis of the ATCA data to avoid the need for scaling. And (3) there may be a very faint extended nebula surrounding the pulsar, and contributing flux density on scales $\geq 40''$, which we have excised but that Burgay et al. (2003) retained. The last scenario is rather unlikely, but cannot be definitively ruled out yet. In any case, the VLA observations, acquired at different times, frequencies, and array configurations, provide a more reliable estimate of the flux density of J0737–3039 itself.

We have thus detected J0737–3039 at 1.6 and 4.8 GHz, derived a spectral index of -2.3 ± 0.2 , and placed an upper limit on its flux density at 8.4 GHz. Orbital modulation due to B is detected in the 1.6 GHz data. Both orbital phase-resolved and phase-averaged measurements at 1.6 GHz are consistent with the entire flux density arising from the pulsed emission of A and B. We find no evidence for unpulsed emission, and limit it to less than 0.5 mJy (5σ). This is a disappointing conclusion for theories that attempted to relate the unpulsed

radio emission and X-ray emission to a common origin in a shock created by the interaction between A and B. If the X-ray emission also turns out to have an “ordinary” origin in the magnetosphere of A, rather than being produced by the interaction between two relativistic winds, then the processes involved in the energy dissipation of neutron stars will have proven more elusive than expected.

We thank Maura McLaughlin, Michael Kramer, and Ingrid Stairs for helping predict the orbital phase of J0737–3039, Joseph Gelfand for assistance with archival ATCA data, Anatoly Spitkovsky and Maxim Lyutikov for helpful discussions, and the anonymous referee for helpful comments. S. C. is a Jansky Fellow of the National Radio Astronomy Observatory (NRAO). NRAO is a facility of the National Science Foundation, operated under cooperative agreement by Associated Universities, Inc.

REFERENCES

- Arons, J., & Spitkovsky, A. 2004, AAS HEAD Meeting, 8, 8.06
 Burgay, M., et al. 2003, *Nature*, 426, 531
 ———. 2005, *ApJ*, 624, L113
 Campana, S., Possenti, A., & Burgay, M. 2004, *ApJ*, 613, L53
 Demorest, P., Ramachandran, R., Backer, D. C., Ransom, S. M., Kaspi, V., Arons, J., & Spitkovsky, A. 2004, *ApJ*, 615, L137
 Kaspi, V. M., Ransom, S. M., Backer, D. C., Ramachandran, R., Demorest, P., Arons, J., & Spitkovsky, A. 2004, *ApJ*, 613, L137
 Lyne, A. G., et al. 2004, *Science*, 303, 1153
 Lyutikov, M. 2004, *MNRAS*, 353, 1095
 Lyutikov, M., & Thompson, C. 2005, *ApJ*, 634, in press
 McLaughlin, M. A., et al. 2004a, *ApJ*, 605, L41
 ———. 2004b, *ApJ*, 613, L57
 ———. 2004c, *ApJ*, 616, L131
 Pellizzoni, A., De Luca, A., Mereghetti, S., Tiengo, A., Mattana, F., Caraveo, P., Tavani, M., & Bignami, G. F. 2004, *ApJ*, 612, L49
 Turolla, R., & Treves, A. 2004, *A&A*, 426, L1